Modeling of the Current Limitations of PEFC

K. Zhukovsky
Faculty of Physics, Moscow State University, Vorobjovy Gory, Moscow 119899, Russia

DOI 10.1002/aic.10853
Published online April 26, 2006 in Wiley InterScience (www.interscience.wiley.com).

PEFC operation in the regime of limiting current has been considered. The phenomenon of oxygen depletion on the cathode is considered responsible for the highest current limits of the cell. The performance of the cell appears to depend strongly on the geometry of the gas diffuser and supply channels. The study of the most promising geometric configurations of the electrodes is carried out. We consider serpentine, interdigitated, and interlaced designs of the gas supply in the electrode. The effect of the geometry on the liquid water removal from the electrode and air pressure in gas channels are studied to identify the best geometry of the gas supply net in terms of the maximum cell current. A comparison between model predictions and experimental data is carried out. © 2006 American Institute of Chemical Engineers *AIChE J,* 52: 2356–2366, 2006
Keywords: transport model, limiting oxygen flux, diffuser, serpentine gas channel and pressure

Introduction

Recent advances in electrochemistry, together with new technologies in manufacturing on the one side and the depletion of oil resources on the planet on the other side, give rise to the wave of interest in alternative sources of energy, such as fuel cells (FC), which convert the chemical energy of hydrogen into electric energy when combined with oxygen. The most popular in the class of FC are probably the polymer electrolyte fuel cells (PEFC), mainly due to their relatively low cost and ease in exploitation. Moreover, this technology is quite flexible in terms of the size of the plants producing electric current, allowing a wide range of output power load and high energy density. PEFCs do not require high operating temperatures and do not present problems with quick start up and component corrosion. Therefore, they are suitable for the needs of transportation. The light weight and compact size of these energy sources, operating at high currents, gathered from a small surface, make these devices especially good for portable devices. The main problem in this case is related exactly to the necessity to gather the highest electric current from the minimal possible surface.

There are three main factors limiting the electric current PEFCs and leading to voltage losses at the output. These factors are activation resistance in the catalyst layer, which is in contact with the electrode and accessible by reacting gases[1-4]; ohmic voltage loss due to the electronic, ionic, and contact resistance of the cell[5-9]; and mass transport resistance. Whereas the new materials and highly effective catalysts and diffusers reduce activation and ohmic resistance, the depletion of the reactant gases on the reaction interface limit the cell performance at high currents, because the gas transport to the reaction sites fails to keep up with the reaction rate. At high current densities, the reaction rate becomes limited mainly by the mass-transfer of the reactant gases, diffusing from the gas channel to the catalyst interfaces through the diffusion layers. This phenomenon regards first of all the oxygen transport, which is additionally obstructed by water vapor production on the cathode. The common way to overcome these limitations is the use of pressured reactants. However, the particular geometry of the gas supply channels can activate additional physical transport mechanisms, which not only improve the gas transport itself, but also help tackle the flood inside the cathode at high currents.

The development of theoretical models of the PEFCs is important for the understanding of the mechanisms of their operation and improvements of their performance So far, numerous theoretical models of PEFC have been developed. Due to advances in the computer sciences, the classical approach to the modeling, which is usually one dimensional, is being sub-

Correspondence concerning this article should be addressed to K. Zhukovsky at zhukovsk@casaccia.enea.it. K. Zhukovsky's current e-mail address is zhukovsk@phys.msu.ru.

stituted by two- and three-dimensional models. Account for the water transport in porous materials becomes common. Some of the works dedicated to the modeling of the PEFC and related topics are given in the reference list.[10-26]

Recently, much attention is being paid to the analysis of the thermodynamics of the cell as well as to the studies of the transport phenomena in cells. The cell potential of the PEFC is evaluated on the basis of potential losses due to the limitations of reactant transport, proton migration, electron conduction, and electrochemical kinetics. Experimental studies demonstrated significant influence of the pressure drops and geometry of supply channels on the effectiveness of the cell (see, for example, refs. 20,21,27,28). Interdigitated serpentine and interlaced configurations of supply channels essentially make use of the pressure driven transport mechanism that complements the molecular diffusion. However, the importance of the development of theoretical models of PEFCs and solving more or less complex systems of mathematical equations is rather in the gain of the understanding of the effect of the operating conditions on cell performance and the conclusions that one derives to undertake right measures and introduce new solutions in the construction or the operating conditions of PEFCs in order to make these devices more efficient. Therefore, careful analysis of the results of a simple model can be important, rather than increasing the complexity of the model.

The present study is focused on the analysis of the phenomena on the cathode in order to understand how the limitations of the PEFC in terms of the maximum current can be overcome. We study oxygen transport, since the current limits come mainly here. At the cathode, the reaction rate is limited by the transport of oxygen from the channels to the catalyst sides and of the water vapor, produced on the catalyst and carried in the opposite direction. In addition to the gas transport limitations, the cathode faces the problem of water flooding due to the massive production of water. The water generation rate at the cathode at high current densities often exceeds its removal rate by the airflow from the inner porous layers. Then the liquid water inside the diffuser layer blocks the pores and obstructs the air supply. This phenomenon is hard to study on the microscopic level because of the inhomogeneity of the microstructure of the carbon diffuser.

The most common approach is that of assuming constant value for the porosity. Moreover, consideration of the non uniformity of the porosity along and across the diffuser and especially the fact that the properties of the gas diffusive layers change with applied compression make its precise mathematical description unreliable. Commonly, the macroscopic model for the essential features of a porous electrode (see, for example, ref. 29) is employed with more or less light modifications. Such an approach is based on the macrohomogeneous description with uniform morphological properties such as porosity, tortuosity, and permeability. It is usually supposed that the water first condenses on the Teflon coated surface in the form of water drops, which, if not carried away, accumulate in puddles, partially or totally obstructing the air supply, leading in this case to the complete flooding of the porous diffuser. The convection transport mechanism contributes to the mass transport, when gas is forced to flow from the gas channels into the diffuser. Being faster in action than diffusion, the convection mechanism increases the reaction rates at the catalyst when the lack of oxygen would otherwise appear. It is important to note that it not only improves the gas supply, but also the shear force of this gas flow field helps remove most of the liquid water gathered into the inner layers of the electrode. Hence, the risk of flooding becomes lower.

The interdigitated channels with closed ends, where gas is forced to flow through the electrode to the exit, make essential use of the effect of the liquid water removal by the shear force of the gas flow. However, it works also in other geometric configurations, such as serpentine and interlaced channels. The disadvantage of the interdigitated gas supply net is in the high flow resistance in such flow design, which results in insufficient airflow, loss of outlet oxygen concentration, and, eventually, in the same insufficient oxygen supply.

Serpentine design combines some of the advantages of the conventional and interdigitated flow fields. Being of open end configuration, the serpentine net allows high air flow rates, whereas the pressure between the serpentine channels, being relatively low, activates the convection mechanism of mass transport, and oxygen transportation to the inner layers of the electrode is executed through both diffusion and convection. The new interlaced configuration of the flow field appears to be the most advanced. It successfully combines the advantages of the serpentine flow field with its high flow rates and interdigitated design, remarkable for its high pressure drops. The complementary action of these two factors results in a significant increase of the performance of the cell at high currents. The easy flow along relatively short gas supply channels effectively removes the water, which gathers in them and at the same time provides the device with the necessary amount of oxygen, well distributed under the whole surface of the diffuser. In its turn, the high pressure drop between the neighboring gas channels, ensured by a special interlaced design of the plate, helps saturate the inner part of the diffuser with oxygen and significantly reduces the flooding in the diffuser. The access of water vapor, which is produced in abundance on the cathode at high electric currents, forms water drops and leads to elevated risk of flood in the body of the diffuser. High pressure drops between the channels induce forced convection in the diffuser, providing the necessary physical mechanism for the removal of water and improving the effectiveness of the oxygen supply in the critical high current regime.

In this work we make use of the simple mathematical model of physical processes in the electrode of PEFCs,[30,31] introducing some minor modifications. We take into account the differences in the pressure drops between the channels of serpentine, interdigitated, and interlaced configurations of gas supply nets; we model the performance of such nets, consisting of 2 to 10 channels. We demonstrate how the new geometric configuration affects the performance of the PEFC. The aim of the studies is to identify the most efficient parameters for various channel configurations. The modeling results are analyzed and compared with experimental results.

Experimental Procedures

Materials

Commercially available 20 wt% Pt/C catalyst powders on carbon black (Vulcan XC72) were purchased from E-Tek Inc. The gas diffusion anode consisted of substrate, diffusive, and catalyst layers. The cathode of 106 cm^2 was prepared using a spray technique described in refs. 32-34. The substrate layer

was based on carbon paper (Toray TGPH090). The weight composition of the diffusion layer was 85 wt% of carbon and 15 wt% of PTFE, with carbon loading of 1.93 mg cm^{-2}. The catalyst layer was prepared by mixing appropriate amounts of carbon-supported catalyst (24.5 wt%) and 5 wt% Nafion ionomer solution from Aldrich (14.9 wt%) and glycerol (60.5 wt%). The platinum loading in all anodes and cathodes was kept constant at 0.34 mg cm^{-2} on the MEA. Nafion 115 membrane (Du Pont) was used after purification treatment in 5 w/v% H_2O_2 solution at 80°C for 1 h, followed by a second treatment in 1 M H_2SO_4. The MEAs were formed by hot pressing the electrodes (106 cm^2) onto the membrane at 130°C for 1-5 min and 50-100 kg cm^{-2}.

Membrane electrode gasket assembly (MEGA) technology[32] was used, and a well-defined shape compatible with the cell hardware was achieved (Figure 1).

This technology allows one to disassemble the cell and to replace the graphite plates, maintaining the same MEA.[32] In this work, aluminum anticorrodal 100 (Alusuisse) end plates (185 mm × 185 mm × 11 mm) were used. At the lateral borders of the assembly and end plates, manifold holes for gas feeding are visible (Figure 1). Graphite flow field plates were assembled with a typical parallel channel configuration of two different types. One of them was composed of 3 parallel channels folded in serpentine on the cathode side and 3 channels on the anode side; the other configuration included 10 channels folded in serpentine on both sides. The commercially available BMA5 graphite, produced by SGL Carbon Group (Germany), was employed for the flow field plates.

Electrochemical characterization

Full-cell electrochemical tests were carried out in the 10 or 3 channel systems using a 106 cm^2 single cell incorporated in a Globe Tech Inc mod. 890 test station. Two aluminum end plates and two graphite current collectors composed the single cell. The MEGA system and the other components of the single fuel cell are schematized in Figure 1.

Cell voltage versus current density measurements were galvanostatically performed with a programmable power supply interfaced with a computer for data acquisition. The results are given in Figures 2a and 2b.[31]

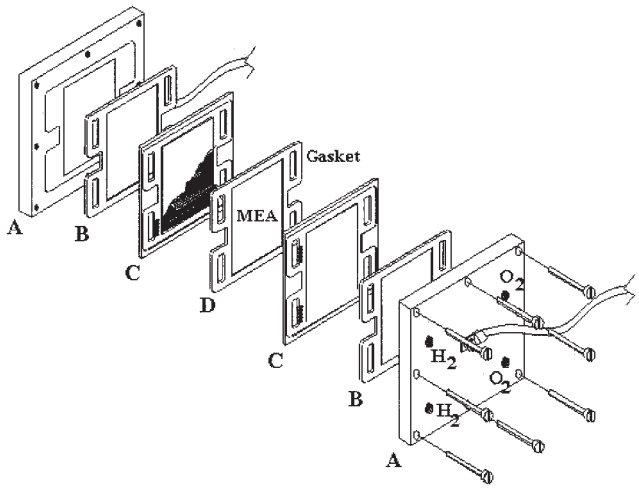

Figure 1. Single PEM fuel cell showing the location of the components.

(A) Aluminum or SS316L end plates, (B) copper current collector/gaskets, (C) graphite flow field plates, (D) MEGA.

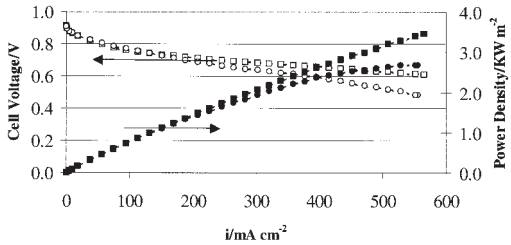

Figure 2. Cell voltage and power density versus current density for 3 (squares) and 10 (circles) cathode channels configuration, at T_{cell} = 75°C under H_2 14 scc/min/A and O_2 52.5 scc/min/A flux at 1.5/1.5 abs bar.

All measurements were carried at 75°C in H_2/O_2 flux at 1.5/1.5 bar absolute pressure.[31] The temperature humidifier was kept at 85°C for the anode and 50°C for the cathode.

Description of the Model

Assumptions

A porous electrode is a complicated structure, and the distribution of micro and macro pores appeared to influence the mass transport characteristic in a very complex way (see, for example, ref. 35). We would need to include a number of parameters to describe the pores in the catalyst layer. Hence, the complete model of the oxygen transport should also imply a large number of parameters. The total effect of the particularities of the distribution of the pores in the carbon paper, diffusive layer, and the catalyst on the oxygen transport is very difficult to estimate. They may vary together with the changes in the carbon material utilized in the electrode. The effects of porosity distribution and variations have been widely discussed in literature.[20,36-39] Moreover, the thermal gradient in actual fuel cells and especially in multi-cell stacks due to the heats of reaction on the electrodes influence effective density and diffusivity coefficients.[26,40] However, it is hardly possible to characterize these gradients precisely. At the same time, it is known that the density-diffusivity product, which characterizes the oxygen transport, varies just a few percent for practical conditions and operating temperatures in a PEFC (see, for example, ref. 7). We assume several simplifications in our attempt to analyze the diffusion effects on fuel cell performances and address current limitations. These are as follows:

- In the absence of water, the porous zones in the fuel cell domain are assumed to be isotropic, with uniform macrocharacteristics such as porosity, tortuosity, and permeability.
- Liquid water modifies the effective porosity (see references and discussion above the bullets).
- We assume isothermal properties for the system and neglect the effect of gravity.
- The gas mixture is considered a perfect gas.
- In the pores of the gas diffuser, we assume that the water vapor is in equilibrium with liquid water in the form of small water drops and liquid water does not constitute a continuous barrier to oxygen transport (see, for example, ref. 41).

• Water leaves the channels and enters the electrode in the form of saturated water vapor only.

• We also assume that the water in the gas diffuser takes off only a negligible amount of dissolved oxygen and nitrogen, compared to the large gas phase.

• The active catalyst layer is assumed to exist only as an ultra thin plane, so that the transport of the reactants within this layer and the gas diffusion in the membrane can be neglected.

• Usually, gas pressures are approximately equal to each other at the anode and the cathode of the PEFC. Moreover, the membrane is practically impermeable for the gas phases. Then the assumption that the pressure varies in the diffusers plane only: $p(x) = const$ is justified.

• The processes in the fuel cell are steady state and the conditions are stationary.

• We also assume that there are no sinks and sources in the body of the diffuser and the electrochemical reaction takes place on the surface of the catalyst layer only.

Such assumptions are commonly made in the literature. In this work we will analyze the influence of various geometric configurations on the high current cell performance, and for our purposes it is enough to consider that:

• The electrochemical processes as well as ion migration and loss factors like ohmic drop in the solid phase are independent of the diffusion processes, which are mainly responsible for the cell limits, and, therefore, we do not include them in the model.

Other assumptions will be discussed as the model equations are presented and the model is applied to the electrode of the polymer electrolyte fuel cell with serpentine gas channel net. How the liquid water is transferred to the cathode is not included in the model.

Governing equations

We employ the equations of the model of K. V. Zhukovsky,[30] where we will account for water flooding. Consider two parallel gas channels, at a distance d under a diffuser of thickness h in the electrode of the polymer electrolyte fuel, as shown on Figure 3.

The spices are transported to the top of the catalyst layer by diffusion and the D'Arcy flow (see, for example, ref. 42). Completing it with the conservation law, we obtain the set of governing equations as written below:

$$\vec{I}_i = -\rho D_i \vec{\nabla} c_A + \rho_i \vec{u},\ \vec{\nabla} \cdot \vec{I}_i = 0,\ \vec{u} = -\frac{\kappa}{\mu}\vec{\nabla} p,$$
$$\sum_i c_i = 1,\ c_i = \rho_i/\rho,\ \rho = pM/RT, \quad (1)$$

where $\vec{I}_i$ are the fluxes of i substances [$kg/m^2 \cdot s$], c_i are their mass fractions, ρ_i are their densities [kg/m^3], ρ is total density [kg/m^3], p is pressure [Pa], D_i is diffusion coefficients of gases into the mixture [m^2/s], $\vec{u}$ is the bulk speed of the gas mixture [m/s], R is the gas constant [J/mol·K], T is temperature [K], k is the permeability coefficient [m^2], μ is the viscosity coefficient [Pa·sec], and M is the molecular mass of the mixture [g/mol]. Further, we shall also use d, the distance between those points [m], and h, the thickness of the diffusive layer [m]; we will use the same units if not noted otherwise.

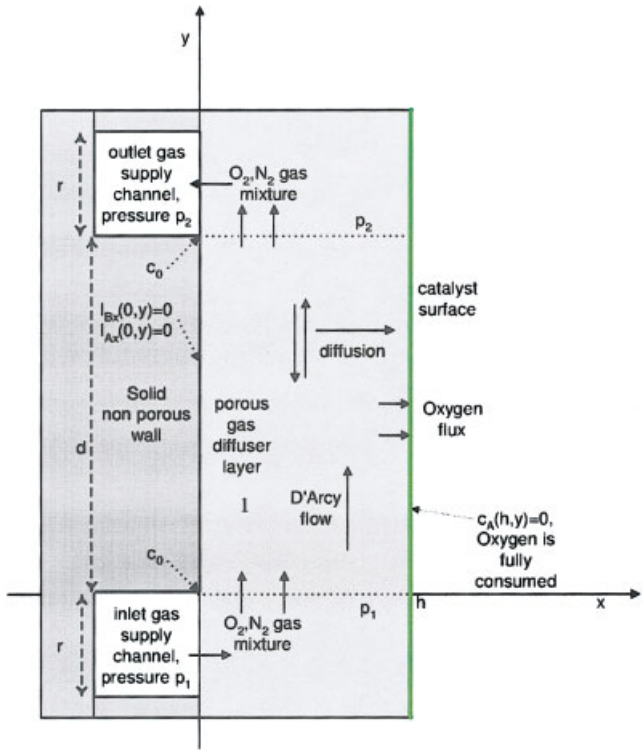

Figure 3. Drawing of an electrode of a polymer electrolyte fuel cell.

[Color figure can be viewed in the online issue, which is available at www.interscience.wiley.com.]

The set of boundary conditions for the case of limiting current is derived from the supposition that the oxygen of initial concentration c_0 is fully converted on the catalyst surface of the PEFC. Then the boundary conditions are written as follows:

$$p = p(y)p(0) = p_1,\ p(d) = p_2,\ I_{i,x}(x = 0,\ y) = 0,\ c_{O2}(h,\ y) = 0,\ c_{O2}(0,\ 0) = c_0,\ c_{O2}(0,\ d) = c_1. \quad (2)$$

The diffusion coefficient D_i is, generally speaking, a function of temperature, pressure, and gas composition. However, the effective diffusion coefficient of oxygen in a nitrogen-water vapor mixture can be calculated as a function of binary diffusion coefficients:

$$D_{O2} = \frac{1 - (x_{O2}M_{O2}/M)}{\dfrac{x_w}{D_{O2-w}} + \dfrac{x_{N2}}{D_{O2-N2}}},\ x_w = \frac{p_w^{sat}}{p},$$
$$c_w = x_w \frac{M_w}{M},\ \sum_i x_i M_i = M, \quad (3)$$

where x_i are the mole fractions, $D_{O2\text{-}w}$ are diffusion coefficients of oxygen in water vapor, $D_{O2\text{-}N2}$ are diffusion coefficients of oxygen in nitrogen, M is the molecular mass of the mixture, M_i is the molecular mass of i substance, and other notations are the

same as in Eq. 1. Water saturation pressure can be found from the following semi-empirical approximation[43]:

$$\ln p_w^{sat} = -5.80022 \times 10^3/T + 1.39150 - 4.86402 \times 10^{-2}(T + 4.176 \times 10^{-5})T^2 - 1.44521 \times 10^{-7}(T^3 + 6.54597)\ln T. \quad (4)$$

It was shown that when the operational temperatures remain low, the binary diffusion coefficients depend on critical temperatures $T_{c,i}$, $T_{c,j}$, pressures $p_{c,i}$, $p_{c,j}$, and masses M_i, M_j of the respective components i and j. They also depend on the total pressure of gas, p, and its temperature, T, as represented by the equation below[44]:

$$pD_{i-j} = a\left(\frac{T}{\sqrt{T_{c,i}T_{c,j}}}\right)^b (p_{c,i}p_{c,j})^{1/3}(T_{c,i}T_{c,j})^{5/12}\left(\frac{1}{M_i} + \frac{1}{M_j}\right)^{1/2}, \quad (5)$$

where $a = 3.640 \times 10^{-4}$, $b = 2.334$ for water-oxygen and water-nitrogen and $a = 3.64 \times 10^{-4}$, $b=1.823$ for oxygen-nitrogen diffusion coefficients. The oxygen concentration in the electrode varies from zero in the catalyst layer to the maximum possible value in saturated humid air. However, with such variation, the change in the density-diffusivity product ρD_{O2} is negligible (less than 4%) under normal fuel cell operation conditions.[7] Then at low pressures and constant temperature, the following combinations of variables are constants:

$$\alpha = pD_{O2}/RT = const,\ \beta = \kappa/\mu RT = const. \quad (6)$$

The presence of water in the form of liquid drops and either mini puddle changes the values of the porosity. We will account for the effective tortuosity and porosity of the diffuser in the simple way through the commonly used by researchers Bruggeman-type correction, which estimates the effective oxygen diffusion coefficient with the following relation:

$$D_{O2}^{eff}i = D_{O2}\varepsilon_i^{1.5}, \quad (7)$$

where D_{O2} is determined by Eq. 3 and ε is the dimensionless porosity factor of the diffuser.

The above-determined problem Eq. 1 with the boundary conditions Eq. 2 has been found to have the following analytical solution for oxygen flux, directed to the catalyst J_{O2} [kg/s^2] (see ref. 30):

$$J_{O2} = \int_0^d I_{Ax}(h, y)dy = \alpha\frac{\pi}{h}\left(\frac{E_1}{H-G}\exp\frac{H-G}{2}y + \frac{E_2}{H+G}\exp\frac{H+G}{2}y\right), \quad (8)$$

where

$$E_1 = \frac{c_0 - c_1\exp\left\{-\frac{G+H}{2}d\right\}}{1-\exp\{-Gd\}}, E_2 = \frac{-c_0\exp\{-Gd\} + c_1\exp\left\{-\frac{G+H}{2}d\right\}}{1-\exp\{-Gd\}}, \quad (9)$$

$$G = \sqrt{4F^2 + H^2},\ F = \frac{\pi}{2h},\ H = -\frac{\beta}{\alpha}\frac{p_2^2 - p_1^2}{2d}. \quad (10)$$

Here p_1 and p_2 are the pressures in the two points of the two channels in question, d is the distance between those points, h is the thickness of the diffusive layer, c_0 is the initial mass fraction of oxygen in the "in" channel, c_1 is the final mass fraction of oxygen in the "out" channel, and α and β are given by Eq. 6.

Then for the entire gas supply net, we obtain the oxygen flux Ω_{O2} [kg/s] by running the model along the channels from the inlet to the outlet and obtain the following expression for the oxygen flux, reaching the catalyst surface over two channels:

$$\Omega_{O2} = \alpha\frac{\pi}{h}\int_0^L dl\left(\frac{E_1(z)e^{\frac{H(z)-G(z)}{2}y}}{H(z)-G(z)} + \frac{E_2(z)e^{\frac{H(z)+G(z)}{2}y}}{H(z)+G(z)}\right), \quad (11)$$

where E_1, E_2, G, H, and F are given by Eqs. 9 and 10; $p_1(z)$ and $c_0(z)$ are the inlet channel pressure and oxygen mass fraction; $p_2(z)$ and $c_1(z)$ are the outlet channel pressure and oxygen mass fraction; α and β are constants given by Eq. 6; d is the distance between the channels; and L is the length of one channel. Hence, the total flux for the whole catalyst surface can be easily obtained by repetitive integration (as discussed above) for each pair of neighboring pair of channels, thus scanning the whole gas supply net.[31]

Flood Correction for the Current Limitations in the PEFC

With the help of the above-described simple model of the oxygen transport in pores of the PEFC, we perform the comparative analysis of the maximum current limitations of the PEFC for serpentine, interdigitated, and interlaced configurations of gas supply channels, holding the comparison between the nets of 2, 3, 4, 5, 7, and 10 parallel channels, machined on a square plate. With the electrochemical processes on the catalyst independent of the gas channel supply configuration, additional losses in the catalyst layer and those due to ohmic resistance being practically equal for all channel configurations, we consider the limiting current of the PEFC determined by the maximum oxygen flow, converted on the catalyst. The pressure regime is set equal for every channel net. The porosity of the medium is taken into account via the effective porosity coefficient, which describes the medium partially filled with liquid water pores, when vapor and water are in thermo- and hydro-dynamic equilibrium. The difference in the amount of water retained by the gas diffuser comes from the different nature of the mass transport in it for different channel configurations. Forced convection, originating from the pressure gra-

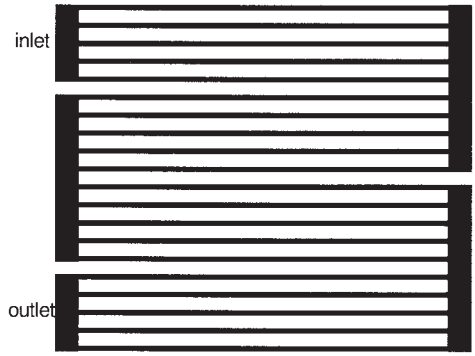

Figure 4. Illustration of n = M × N parallel channels serpentine configuration of gas supply channels in a PEFC.

dient between the neighboring serpentine sections, helps remove the majority of water from the diffuser in that area. Where the gas channels lay, a certain part of the liquid water is removed from the diffuser just over them due to the channel gas flow. The diffuser over the shoulders between the channels within a section of the serpentine is supposed to be flooded more, since the water neither finds its immediate exit to the gas channel, nor does convection contribute to its removal because of the absence of the pressure drop between such channels.

Although it is hard to measure and obtain precise information about the quantities of liquid water in various points of the diffuser, we suppose that the water reduces the volume of the pores in the diffuser by maximum a quarter, whereas the removal of the water by convection is complete. It is not worth taking into consideration the higher grades of flood in the framework of the current approach, since as soon as the water drops form a puddle, the mechanism of flooding that we imply cannot be described correctly on the phenomenological level. Therefore, our approach remains limited to such a case of moderate flood.

Consider the serpentine configuration, schematically given on Figure 4.

First, we consider the constant air flux regime, which is sometimes used in simple constructions of PEFC electrodes, which are aimed at lowering the production costs (one of the reasons that stop this technology from winning on the energy production market) rather than at beating records in performance. Modeling air flows through the diffuser of PEFC over 2, 3, and 10 serpentine gas supply channels evidenced the higher values of the maximum oxygen catalyst flux for a smaller number of channels in section.[31] The maximum oxygen flow to the catalyst increases *15-20%* for 3 and 2 channel serpentine, respectively, to 10 channel net, when evaluated regardless of the water flood. Consequently, the relative increase of the limiting current of the cell follows. Some more complex designs operate with fixed inlet pressure and the air flux in the gas supply channel, following the electric current, produced by the cell. Such a method provides the electrode with plenty of oxygen for nearly all reasonable currents. The predictions for such regime with the air flux $\approx 40 \times 10^{-6} m^3/min/A$ also result in 13% limiting oxygen flux increase for 3 channel serpentine, respective to the 10 channel design (see ref. 31).

The high impact of the porosity and flood in the diffuser on the cell performance has been recognized by researchers.[36] Considering three different domains of the diffuser—those over the channel, between the channels within a section, and between the sections of the serpentine-we can assume constant porosity coefficients, the highest-$\varepsilon_1 = 0.8$-over the channel and the lowest-$\varepsilon_3 = 0.55$-between the sections of the serpentine.[20] The modeling results are given in Table 1. Furthermore, we can adopt the simple dynamic model of the flooding effect in the electrode. There are very few data on the change of the porosity in the gas diffusion layer, particularly in the presence of water in it. The few existent hypotheses propose linear or exponential functions for porosity (see, for example, refs. 22 and 38). We consider the flood in the diffuser with the supposition that the percentage of the pores available for gas transport depends on the pressure gradient so that effective porosity varies from $\varepsilon_1 = 0.8$ when all the water is removed by the shear flow to $\varepsilon_1 = 0.55$ when the shear flow is absent. Our approach results in the predictions given in Table 1.

Table 1. Relative Increment of the Limiting Current Due to Oxygen Transport Limitations in the Partially Flooded Model in *N* Channel Serpentine Respective to 10 Channel Serpentine for Constant Air Flow to Electric Current Ratio

M Channels N Sections	M = 10 N = 5 $P_1 = 1.6 \cdot 10^6$ Pa	M = 7 N = 7 $P_1 = 1.6 \cdot 10^6$ Pa	M = 5 N = 10 $P_1 = 1.6 \cdot 10^6$ Pa	M = 4 N = 13 $P_1 = 1.7 \cdot 10^6$ Pa	M = 3 N = 17 $P_1 = 1.7 \cdot 10^6$ Pa	M = 2 N = 25 $P_1 = 1.7 \cdot 10^6$ Pa
Max current ratio: $I_{M\,ch}$ to I_{10ch} (%) for airflow $\approx 50 \cdot 10^{-6}$ m^3/min/A.	0%	4%	9%	15%	23%	39%
Max current ratio: $I_{M\,ch}$ to I_{10ch} (%) for airflow $\approx 90 \cdot 10^{-6}$ m^3/min/A.	0%	4%	10%	15%	24%	Too high pressure drop
Max current ratio: $I_{M\,ch}$ to I_{10ch} (%) for airflow $\approx 90 \cdot 10^{-6}$ m^3/min/A. DYNAMIC MODEL	0%	4%	10%	16%	25%	Too high pressure drop
Max current ratio: $I_{M\,ch}$ to I_{10ch} (%) for airflow $\approx 50 \cdot 10^{-6}$ m^3/min/A. DYNAMIC MODEL	0%	3%	8%	13%	22%	40%

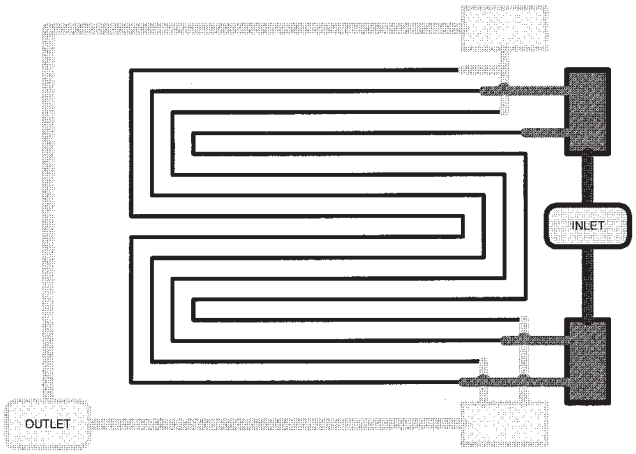

Figure 5. Illustration of interlaced configuration of n parallel gas channels in a PEFC.

It follows from Table 1 that, by taking into account the liquid water present in the pores, the limiting oxygen flow increase for $m = 3$ channels against $m = 10$ in serpentine exceeds *20%*. The pressure regime is chosen so that the airflow in the channels is independent of the channel configuration. In particular, the airflow $\approx 40 \times 10^{-6} m^3/min/A$. and $\approx 90 \times 10^{-6} m^3/min/A$. was set. Variations in the air flow affects the predictions for the maximum catalyst oxygen flux only slightly. The model is not sensitive to the type of the function for the porosity. Indeed, with air flux and pressure drop, increasing twice, we observe a difference of just a few percent in maximum currents. Despite the calculations being done with the exponential function for the porosity, there is just little percent change in the result coming due to the pressure increase, which means choosing linear approximation instead of exponential is possible. However, the right pressure regime is important from a practical point of view, since it may be difficult to maintain the air supply, following the current, for some channel sets. For example, the 2-3 channels in serpentine require a high pressure drop, which increases the costs of the cell and makes the construction more complex.

Table 2. Geometric Parameters of the Channels (channel width r [m/100] and distance between channels d[m/100])

r = channel width	0.05	0.06667	0.1	0.13333	0.15
d = distance between channels	0.15	0.13333	0.1	0.06667	0.05

The Effect of the Air Supply Channel Width and the Distance Between the Channels on the Current Limitations in PEFC with Serpentine Gas Supply Net and New Interlaced Gas Supply Net

Now let us consider, in particular, the interlaced geometric configuration of the gas supply channels in PEFC, schematically given in Figure 5, and compare its performance at high currents with the serpentine in Figure 4.

We will consider the moderate flood in the diffuser when the effective porosity varies from $\varepsilon_1 = 0.8$ to $\varepsilon_1 = 0.55$, which means that approximately 30% of pores are flooded. Higher grades of flood are extremely difficult to model due to the nature of the phenomenon, when the excessive amount of water in the form of separate drops starts forming puddles in the diffuser, thus unpredictably changing the porous distribution and spontaneously blocking the air supply. In the preceding sections we assumed the air channel width r equal to the distance between the channels $d = 0.001m$. Now, let's investigate the effect of the geometric ratio of *r/d* on the effectiveness of the cells with both serpentine and interlaced air supply nets, considering the following set of r and d, collected in Table 2:

Modeling yields the results collected in Tables 3 and 4.

The elaboration of the data for the limiting air fluxes of the cells with the interlaced and serpentine air supply nets definitely indicates better performance of the interlaced configuration practically for every ratio of *r/d* in the considered range of *1/3-3*. The comparison of limiting oxygen flux of the configurations in question reveals more than *20%* advantage of the interlaced gas net over the serpentine one for the best performing serpentine design with $r/d = 2 \div 3$, that is, with $r = 0.133 \cdot 10^{-2} m$, $d = 0.067 \cdot 10^{-2} m$, and $r = 0.15 \cdot 10^{-2} m$, $d = 0.05 \cdot 10^{-2} m$. The preferable ratio for the interlaced channel appears to be $r/d = 1/2 \div 1/3$ that is, with $d = 0.133 \cdot 10^{-2} m$, $r = 0.067 \cdot 10^{-2} m$, and $d = 0.15 \cdot 10^{-2} m$, $r = 0.05 \cdot 10^{-2} m$.

Table 3. Limiting Catalyst Oxygen Flux and Relative Increment of the Limiting Current for $\Delta P_{ref} = 0.075 \times 10^6$ Pa

	N = 5 M = 10 P_1 = 1.6 Δp = 0.075	N = 7 M = 7 P_1 = 1.6 Δp = 0.135	N = 10 M = 5 P_1 = 1.6 Δp = 0.27	N = 13 M = 4 P_1 = 1.7 Δp = 0.463	N = 7 M = 3 P_1 = 1.7 Δp = 0.85	r/d
Ratio	2.6	2.7	2.6	2.4	2.1	
Serpentine	0.02340	0.02549	0.02854	0.03157	0.03625	
Interlaced	0.06116	0.06838	0.07370	0.07649	0.07775	1/3
Ratio	2.3	2.3	2.2	2.1	1.9	
Serpentine	0.02742	0.02941	0.03222	0.03495	0.03918	
Interlaced	0.06181	0.06793	0.07234	0.07460	0.07567	1/2
Ratio	1.7	1.8	1.7	1.7	1.6	
Serpentine	0.03539	0.03704	0.03924	0.04129	0.04449	
Interlaced	0.06164	0.06575	0.06858	0.06998	0.07070	1
Ratio	1.4	1.4	1.4	1.4	1.3	
Serpentine	0.04297	0.04412	0.04556	0.04686	0.04889	
Interlaced	0.05952	0.06195	0.06356	0.06431	0.06475	2
Ratio	1.2	1.3	1.3	1.2	1.2	
Serpentine	0.04630	0.04715	0.04819	0.04911	0.05054	
Interlaced	0.05780	0.05952	0.06064	0.06115	0.06146	3

Table 4. Limiting Catalyst Oxygen Flux and Relative Increment of the Limiting Current for $\Delta P_{ref} = 0.035 \times 10^6$ Pa

	N = 5 M = 10 P_1 = 1.6 Δp = 0.035	N = 7 M = 7 P_1 = 1.6 Δp = 0.063	N = 10 M = 5 P_1 = 1.6 Δp = 0.126	N = 13 M = 4 P_1 = 1.7 Δp = 0.216	N = 17 M = 3 P_1 = 1.7 Δp = 0.397	N = 25 M = 2 P_1 = 1.75 Δp = 0.85	r/d
Ratio	2.2	2.4	2.5	2.4	2.2	1.8	
Serpentine	0.02255	0.02410	0.02643	0.02895	0.03316	0.04155	
Interlaced	0.04970	0.05853	0.06638	0.07065	0.07292	0.07299	1/3
Ratio	1.9	2.1	2.2	2.1	2.0	1.6	
Serpentine	0.02667	0.022819	0.03039	0.03270	0.03653	0.04414	
Interlaced	0.05196	0.05963	0.06626	0.06977	0.07165	0.07175	1/2
Ratio	1.6	1.7	1.7	1.7	1.6	1.4	
Serpentine	0.03485	0.03618	0.03796	0.03973	0.04266	0.04845	
Interlaced	0.05488	0.06024	0.06468	0.06688	0.06807	0.06823	1
Ratio	1.3	1.3	1.4	1.4	1.3	1.2	
Serpentine	0.04265	0.04361	0.04480	0.04593	0.04778	0.05144	
Interlaced	0.05550	0.05875	0.06135	0.06256	0.06323	0.06339	2
Ratio	1.2	1.2	1.2	1.2	1.2	1.2	
Serpentine	0.04608	0.04679	0.04765	0.04844	0.04975	0.05231	
Interlaced	0.05496	0.05728	0.05911	0.05994	0.06040	0.06053	3

The serpentine configuration is more sensitive to the choice of the ratio *r/d* than the interlaced one. Changing the value of *r/d* from *r/d = 2 ÷ 3* to *r/d = 1/2 ÷ 1/3*, we obtain a *30%* decrease of the limiting oxygen flux, whereas the flux for the interlaced net gains *22%*. Serpentine net with such values *r/d = 1/2 ÷ 1/3* fails to deliver oxygen to the catalyst effectively, and interlaced configuration becomes twice as effective. Analyzing the effectiveness of both gas supply configurations for the number of channels, folded in serpentine or interlaced, we note that the efficiency is higher with the 2 and 3 channel configurations. Moreover, for fixed *r/d = 1/2* or *1/3*, the limiting oxygen flux is much more sensitive to the change of the number of channels in the folder than for *r/d = 2 ÷ 3*. The maximum oxygen flux Ω decreases *30%* for both configurations when scaling up from 3 to 10 folded channels for $d = 0.15 \cdot 10^{-2} m$, $r = 0.05 \cdot 10^{-2} m$, as illustrated in Figures 6 and 7.

With the set of parameters *d = 0.05cm*, *r = 0.15cm,* we find the maximum oxygen flux Ω less sensitive to the number *M* of channels in sections. It decreases just *8-9%* for 10 channels in the folder, respectively to 3 channels in the folder. Moreover, comparing corresponding Figures 6 and 7, we notice that the increase of the pressure in the channels makes the limiting current less dependent on all the geometric parameters for any configuration.

Eventually, Figures 8 and 9 illustrate the common effect of the geometric ratio of the channel width *r* to the distance between the neighboring channels *d* and the number of channels *M*, folded in sections for serpentine and interlaced configurations.

The diagrams evidence that the highest limits on the maximum current are obtained with the interlaced gas supply net with the channels width $r = 0.15 \div 0.1 \cdot 10^{-2} m$, the distance between the neighboring channels $d = 0.05 \div 0.1 \cdot 10^{-2} m$, and the number of the channels, folded in sections *M = 2 or 3*. However, *4, 5,* and *7* channel nets demonstrate low dependence on *r/d* and just some *10%* lower performances. Serpentine net performance depends strongly on the geometric parameters and sets competitively high limits on the maximum current when it consists of *3* or, better, *2* channels in serpentine and the ratio *r/d > 1*.

Discussion and Conclusions

Our measurements evidenced *25%* higher cell current for 3 channel serpentine against 10 channel configurations in the

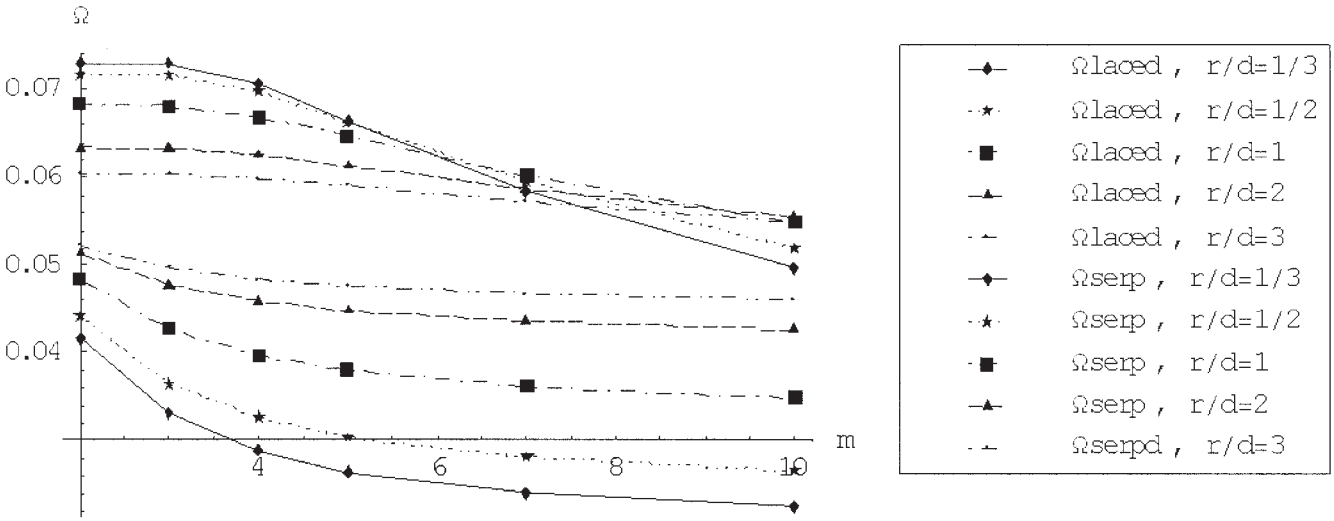

Figure 6. Limiting catalyst oxygen flux Ω (relative units) for $\Delta P_{ref} = 0.035 \times 10^6$ Pa.

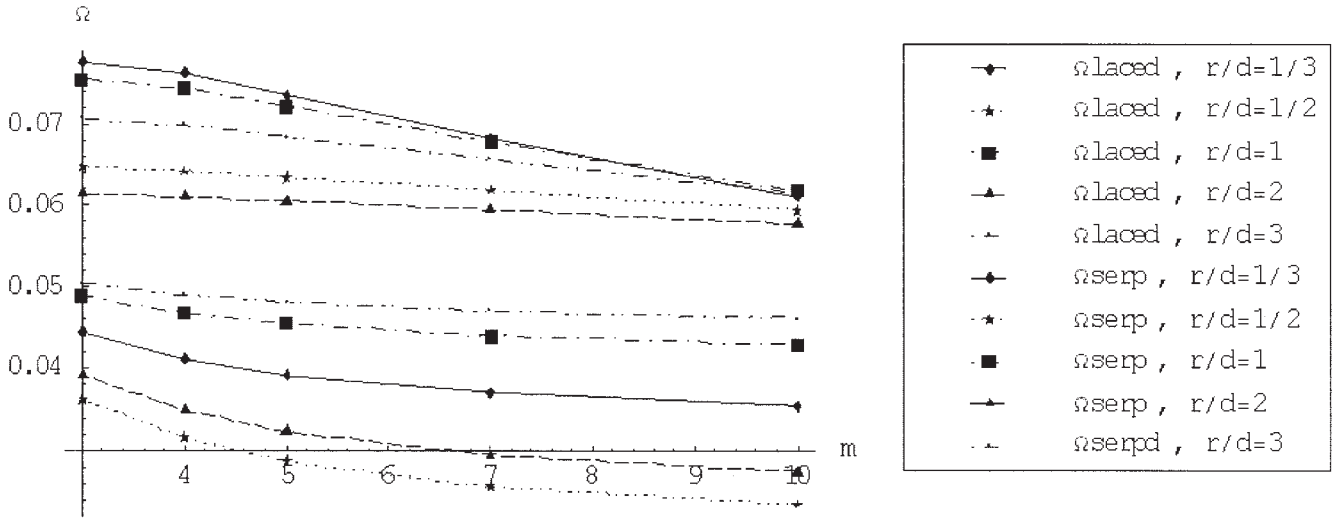

Figure 7. Limiting catalyst oxygen flux Ω (relative units) for $\Delta P_{ref} = 0.075 \times 10^6$ Pa.

high current regime, when the air flow in air supply channels followed the produced electric current at *52 cm³/min/A* (the maximum current was limited at *0.6 A/cm²* due to technical reasons). Theoretical predictions also demonstrate that the efficiency of the PEFC at high currents increases with the decrease of the number of supply channels in a serpentine section–*M*. However, in order to maintain the equal air supply for all configurations, the high pressure drop Δp is needed for serpentines of *3* and, in particular, *2* channels, folded. The predictions of the model, accounting for the effect of liquid water, are in good agreement with the measured values of the maximum current increase. Such increase appears because of the high pressure drop Δp between the sections of the serpentine with *2* and *3* channels in the folder, which stimulates the air flow in the diffuser between the channels of neighboring sections and adds forced convection to the molecular diffusion in the matter. We note that the limiting current slightly increases with the rise of the pressure.

The new interlaced configuration of the gas supply net shows better performances than common serpentine configurations, practically for any ratio of *r* and *d* in the range from *1/3* to *3*, gaining more than *20%* of the limiting current in any case. The serpentine channel net reaches the best performance with $r/d \sim 2$ or *3*. The interlaced net is most effective at $r/d \sim 1/2$ or *1/3*. Varying the geometric ratio *r/d* from $r/d = 3$ to $r/d = 1/3$, we obtain *30%* decrease of the limiting oxygen flux for the serpentine design, whereas the flux for the interlaced net gains *22%*. The analysis of the effectiveness of the air supply con-

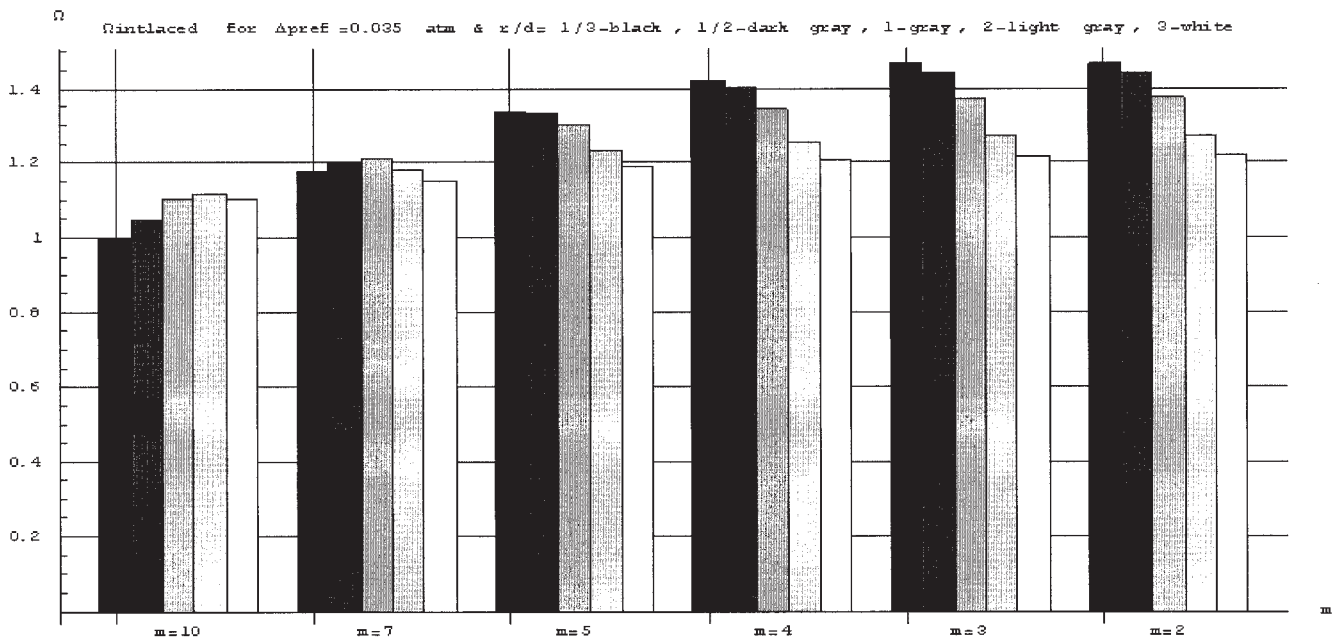

Figure 8. Limiting catalyst oxygen flux of interlaced channel net, normalized on the flux for the reference 3 channel serpentine for r/d and M.

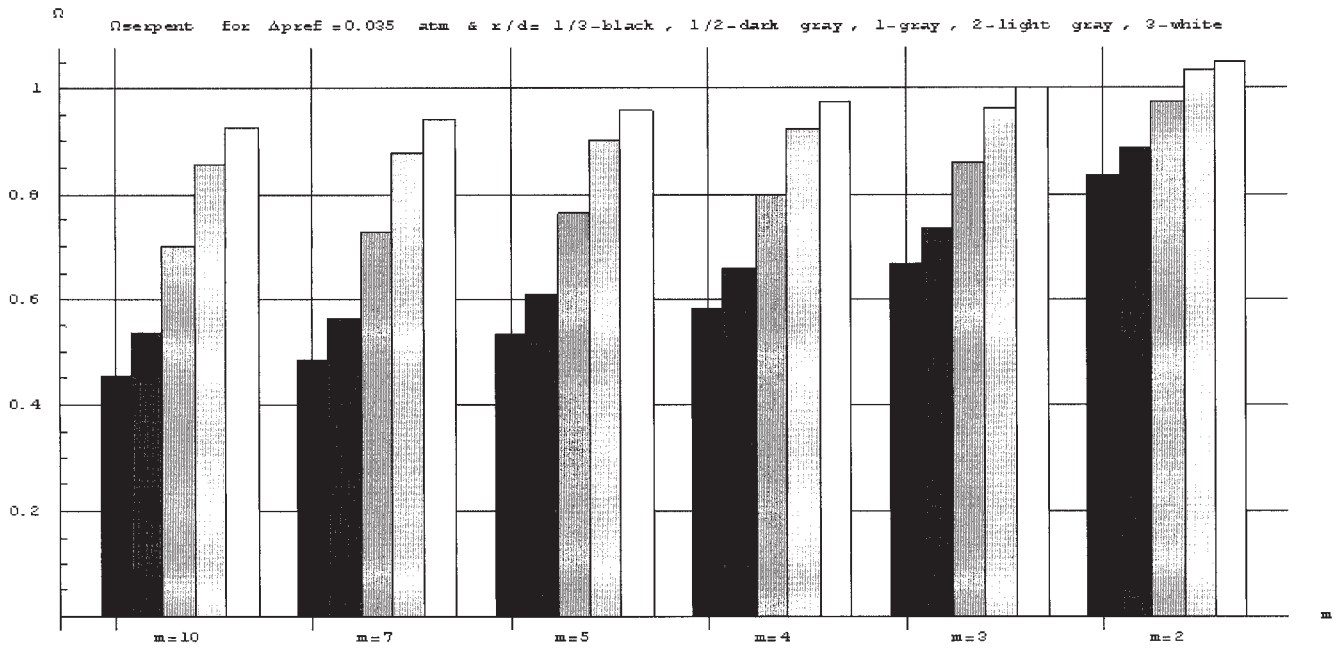

Figure 9. Limiting catalyst oxygen flux of serpentine channel net, normalized on the flux for the reference 3 channel serpentine for r/d and M.

figurations for the number of channels, folded in common or interlaced serpentine, indicates that the most efficient are the 2 and 3 channel configurations. However, the 2 channel net requires high pressure drops for proper operation, and it makes the device more expensive and less reliable in the long term. Moreover, it may not always be possible to provide such a regime due to technical reasons. Since the 2 channel interlaced net provides just slightly higher maximum current than 3 and 4 channel nets, the last ones are preferable due to higher reliability and ease of exploitation.

The common serpentine configuration is also a suitable solution for a low cost air supply in PEFCs, although their performance is sensitive to the choice of the ratio *r/d*. The serpentine net with values $r/d = 1/2 \div 1/3$ fails to deliver oxygen to the catalyst effectively, while the interlaced configuration results are twice as effective. It is important to underline that although the maximum current is highest for the 2 channel net configuration, in order to obtain the required air flux, the pressure drop should be at least $\Delta P_{2chan.net} \sim 0.85 \times 10^6 Pa$. Due to technical difficulties at high pressure air supply, the inlet pressure was fixed at $P_1 \approx 1.6 \times 10^6$ *Pa*.

The results obtained and discussed above lead to the following conclusions:

- Due to the full use of the forced convection mechanism, the interlaced gas supply channel net is preferable to the common serpentine net. The net of few interlaced channels provides the best oxygen supply for the electrode, exceeding that of the common serpentine by 20% to 40% and consequently increasing the limit on the maximum current.
- Interlaced gas supply nets of *2*, *3*, or *4* channels of $r = 0.15 \div 0.1 \times 10^{-2} m$ width, with the distance between the neighboring channels $d = 0.05 \div 0.1 \times 10^{-2} m$, are recognized as the most suitable for the cell, exploited in the high current regime.
- The serpentine net performance is sensitive to geometric parameters. It performs competitively mainly at high pressures, when it consists of 3 or, possibly, 2 channels in serpentine with the channel width exceeding the distance between them: $r/d > 1$.
- The negative effect of water flood in the diffuser is particularly reduced in the interlaced net and the 2 channels serpentine net. However, the usage of 1-2 channel serpentine is unfavorable because of significant depletion of oxygen along the channels and the necessity of high pressure drops between the inlet and the outlet.
- Dynamic modeling of flooding, accounting for liquid water removal by shear gas flow in the diffuser, dependent on the pressure gradient, predicts better performance of the PEFC working with higher pressure and pressure drop.

Literature Cited

1. Wilson MS, Gottesfeld S. High performance catalyzed membranes of ultra low Pt loadings for PEFC. *J Electrochem Soc.* 1992;139:L28–L32.
2. Taylor EJ, Anderson EB, Vilambi NRK. Preparation of high-platinum-utilization gas diffusion electrodes for PEM fuel cells. *J Electrochem Soc.* 1992;139:L45–L50.
3. Kumar GS, Raja M, Parthasarathy S. High performance electrodes with very low platinum loading for polymer electrolyte fuel cells. *Electrochim Acta.* 1995;40:285–291.
4. Ralph TR, Hards GA, Keating JE, Campbell SA, Wilkinson DP, Davis M, St-Pierre J, Johnson MC. Low cost electrodes for PEM fuel cells. *J Electrochem Soc.* 1997;144:3845–3852.
5. Nguyen TV, White RE. A water and heat management model for PEM fuel cell. *J Electrochem Soc.* 1993;140:2178–2188.
6. Springer TE, Zawodzinski TA, Wilson MS, Gottesfeld S. Characterization of polymer electrolyte fuel cells using AC impedance spectroscopy. *J Electrochem Soc.* 1996;143:N2, 587–595.
7. Toda T, Igarashi H, Watanabe M. Role of electronic property of Pt and Pt alloys on electrocatalytic reduction of oxygen. *J Electrochem Soc.* 1998;145:N12, 4185–4198.
8. Wainright JS, Wang J-T, Weng D, Savinell RF, Litt M. Acid doped

polibenzimidazoles: a new polymer electrolyte. *J Electrochem Soc.* 1995;142:L121–L123.
9. Watanabe M, Satoh Y, Shimura C. Management of water content in polymer electrolyte membranes with porous fibre wicks. *J Electrochem Soc.* 1993;140:N11, 3190–3196.
10. Perry ML, Newman J, Cairns EJ. Mass transport in gas-diffusion electrodes: a diagnostic tool for fuel-cell cathodes. *J Electrochem Soc.* 1998;145:N1, 5–9.
11. Rho YW, Srinivasan S, Kho YT. Mass transport phenomena in proton exchange membrane fuel cells using O_2/He, O_2/Ar, and O_2/N_2 mixtures. *J Electrochem Soc.* 1998;141:N8, 2089–2096.
12. Natarajan D, Nguyen TV. A two-dimensional two-phase multi-component transient model for the cathode of a proton exchange membrane fuel cell, using conventional gas distributors. *J Electrochem Soc.* 2001;148:N12, A1324–A1335.
13. Um S, Wang C-Y, Chen KS. Computational fluid dynamics modelling of proton exchange membrane fuel cells. *J Electrochem Soc.* 2000; 147:4485–4493.
14. Wang ZH, Wang CY, Chen KS. Two-phase flow and transport in the air cathode of proton exchange membrane fuel cells. *J Power Sources.* 2001;94:N1, 40–50.
15. Bering T, Lu DM, Djilali N. Three-dimensional computational analysis of transport phenomena in a PEM fuel cell. *JPower Sources.* 2002;106:284–298.
16. Dutta S, Shimpalee S, Van Zee JW. Numerical prediction of mass-exchange between cathode and anode channels in a PEM fuel cell. *Int J Heat Mass Transfer.* 2001;44:2029–2040.
17. Shimpalee S, Glandt J, Greenway S, Lee WK, Wan Zee J. Proceedings of the Centennial Meeting of the Electrochemical Society, Abstract N 1135, Philadelphia, PA, 2002.
18. Mishra V, Yang F, Pitchumsni R. Analysis and design of PEM fuel cells. *J Power Sources.* 2005;141:47–64.
19. Jansen GJM. A phenomenological model of water transport in a proton exchange membrane fuel cell. *J Electrochem Soc.* 2001;148:N12, A1313–A1323.
20. Gurau V, Barbir F, Liu H. An analytical solution of a half-cell model for PEM fuel cells. *J Electrochem Soc.* 2000;147:N7, 2468–2473.
21. He W, Yi JS, Nguyen TV. Two-phase flow model of the cathode of PEM fuel cells using interdigitated flow fields. *AIChE J.* 2000;46:N10, 2053–2061.
22. Hsuen H-K. Performance equations of polymer electrolyte fuel cells. *J Power Sources.* 2004;126:46–57.
23. Mirzazedeh J, Saievar-Iranizad E, Nahavandi L. An analytical approach on effect of diffusion layer on ORR for PEMFCs. *J Power Sources.* 2004;131:194–199.
24. Rowe A, Li X. Mathematical modelling of proton exchange membrane fuel cells. *J Power Sources.* 2001;102:82–96.
25. Arato E, Bosio B, Costa P, Parodi F. Preliminarily experimental and theoretical analysis of limit of performance of molten carbonate fuel cells. *J Power Sources.* 2001;102:74–81.
26. Ju H, Meng H, Wang C-Y. A single phase, non-isothermal model of the PEM fuel cells. *Int J Heat Mass Transfer.* 2005;48:1303–1315.
27. Nguyen TV. A gas distribution design for PEM fuel cells. *J Electrochem Soc.* 1996;143:L103–L109.
28. Yi JS, Nguyen TV. An along the channel model for proton exchange membrane fuel cells. *J Electrochem Soc.* 1998;145:1149–1155.
29. Newman J, Tiedemann W. Porous-electrode theory with battery applications. *AIChE J.* 1975;21:25.
30. Zhukovskii KV. Three dimensional model of gas transport in a porous diffuser of a polymer electrolyte fuel cell. *AIChE J.* 2003;49:N12, 3029–3036.
31. Zhukovskii KV, Pozio A. Maximum current limitations of the PEM fuel cell with serpentine gas supply channels. *J Power Sources.* 2004; 130:95–105.
32. Pozio A, Giorgi L, De Francesco M, Silva RF, Lo Presti R, Danzi A. Membrane Electrode Gasket Assembly (MEGA) technology for polymer electrolyte fuel cells. *J Power Sources.* 2002;112/2:491–500.
33. Giorgi L, Antolini E, Pozio A, Passalacqua E. Influence of the PTFE content in the diffusion layer of low-pt loading electrodes for polymer electrolyte fuel cells. *Electrochim Acta.* 1998;43:3675–3681.
34. Pozio A, Giorgi L, Antolini E, Passalacqua E. Electroxidation of H_2 on Pt/C Pt–Ru/C and Pt–Mo/C anodes for polymer electrolyte fuel cell. *Electrochim Acta.* 2000;46:555–564.
35. Prasanna M, Ha HY, Ha HY, Cho EY, Hong S-A, Oh I-H. Influence of the cathode gas diffusion media on the performance of the PEMFCs. *J Power Sources.* 2004;131:147–154.
36. Roshandel R, Farhanieh B, Saievar-Iranizad E. The effect of porosity variation on PEM fuel cell performance. *Renewable Energy.* 2005;30: 1557-1572.
37. Lee HK, Park J-H, Kim D-Y, Lee TH. A study of the diffusion layer thickness and porosity of the PEMFC. *J Power Sources.* 2004;131: 200-206.
38. Chu H-S, Chung Y, Chen F. Effects of porosity of the gas diffuser on performance of the proton exchange membrane fuel cell. *J Power Sources.* 2003;123:1-9.
39. Hsuen H-K. Performance of the cathodes in polymer electrolyte fuel cells with non-uniform water flooding in gas diffusers. *J Power Sources.* 2004;137:183-195.
40. Hackenjos A, Muenter H, Wittstadt U, Hebling C. *J Power Sources.* 2004;131:213-216.
41. Eikerling M, Kornyshev AA. Modelling the performance of the cathode catalyst layer of polymer electrolyte fuel cells. *J Electroanal Chem.* 1998;453:89–97.
42. White FM. *Viscous Fluid Flow.* New York: McGraw Hill; 1991.
43. *ASHRAE Handbook: Fundamentals*. American Society of Heating, Refrigerating and Air Conditioning Engineers, Inc.; 2005. ISBN/ISSN 1-931862-71-0.
44. Bird RB, Steward WE, Lighfoot EN. *Transport Phenomena.* New York: Wiley; 1960.

Manuscript received Dec. 20, 2004, and revision received Feb. 22, 2006.